

The University of San Francisco
USF Scholarship: a digital repository @ Gleeson Library |
Geschke Center

Chemistry Faculty Publications

Chemistry

2002

Experimental and Computational Study of the New Gaseous Molecules OMnF and OMnF[Sub 2]

G Balducci

M Campodonico

G Gigli

Giovanni Meloni

University of San Francisco, gmeloni@usfca.edu

S N. Cesaro

Follow this and additional works at: http://repository.usfca.edu/chem_fac

 Part of the [Chemistry Commons](#)

Recommended Citation

Balducci, G.; Campodonico, M.; Gigli, G.; Meloni, G.; Cesaro, S. Nunziante. Experimental and computational study of the new gaseous molecules OMnF and OMnF[sub 2]. *Journal of Chemical Physics*. 12/15/2002, Vol. 117 Issue 23, p10613.

This Article is brought to you for free and open access by the Chemistry at USF Scholarship: a digital repository @ Gleeson Library | Geschke Center. It has been accepted for inclusion in Chemistry Faculty Publications by an authorized administrator of USF Scholarship: a digital repository @ Gleeson Library | Geschke Center. For more information, please contact repository@usfca.edu.

Experimental and computational study of the new gaseous molecules OMnF and OMnF₂

G. Balducci, M. Campodonico, and G. Gigli^{a)}

Dipartimento di Chimica, Università di Roma "La Sapienza," p.le A. Moro 5, 00185 Roma, Italy

G. Meloni

Department of Chemistry, University of California, Berkeley, California 94720

S. Nunziante Cesaro

CNR—Istituto per lo Studio dei Materiali Nanostrutturati, Sezione Roma 1, c/o Dipartimento di Chimica, Università di Roma "La Sapienza," p.le A.Moro 5, 00185 Roma, Italy

(Received 5 August 2002; accepted 19 September 2002)

The new gaseous species OMnF and OMnF₂ were identified and studied by high-temperature Knudsen Cell Mass Spectrometry. Their thermochemical atomization energies were derived through the study of several all-gas equilibria in the temperature range 1735–1913 K. FTIR matrix isolation experiments together with *ab initio* and density functional calculations were performed to determine the molecular parameters, bond distances, and vibrational frequencies of OMnF_(g) and OMnF_{2(g)}. The results allowed us to evaluate a set of thermal functions for the new species that were used in the evaluation of the equilibrium data. The proposed atomization energies and enthalpies of formation are $\Delta_a H_0^\circ(\text{OMnF}, g) = (903 \pm 5) \text{ kJ mol}^{-1}$, $\Delta_f H_{298.15}^\circ(\text{OMnF}, g) = (-297 \pm 5) \text{ kJ mol}^{-1}$, and $\Delta_a H_0^\circ(\text{OMnF}_2, g) = (1470 \pm 70) \text{ kJ mol}^{-1}$, $\Delta_f H_{298.15}^\circ(\text{OMnF}_2, g) = (-789 \pm 70) \text{ kJ mol}^{-1}$. © 2002 American Institute of Physics. [DOI: 10.1063/1.1520141]

I. INTRODUCTION

In contrast to the corresponding binary halides and oxides the thermodynamic and spectroscopic properties of the ternary gaseous oxyhalides of the first transition series metals have been scarcely investigated. These species may be formed through gas–solid reactions, where a relatively unvolatile oxide phase and a more volatile halide of the same metal interact at high temperatures to yield the gaseous oxyhalide species. Knowledge of the formation conditions and the thermodynamic stability of these volatile species are of concern in chemical equilibrium modeling of various chemical transport processes such as high-temperature materials corrosion, pyrometallurgy, and, more recently, in halide lamp systems.

As concerns, in particular, the O–Mn–F system, some molecular constants and vibrational features were reported previously for the species O₃MnF(g).^{1–4} No thermochemical data were available.

In the research reported here thermochemical information for the two new gaseous species OMnF and OMnF₂ was obtained from the Knudsen cell-mass spectrometric (KC-MS) measurement of a number of all-gas equilibria involving these species. Concurrently, some vibrational features of the same OMnF and OMnF₂ species were obtained from FTIR-matrix isolation experiments for which the trapped vapor species were produced in effusive conditions similar to those of the KC-MS experiments. Some very preliminary experimental results have been anticipated in Ref. 5. In this paper, the completed experiments were complemented with

ab initio and density functional (DF) calculations to provide reliable molecular parameters subsequently used in the evaluation of the thermal functions of the species under study.

II. EXPERIMENT

A. Mass spectrometry

Knudsen cell-mass spectrometry has been employed in this investigation. This classical technique continues to be an invaluable tool for the identification and thermochemical characterization of new gaseous molecules. The basic features of the technique have been previously described.^{6,7} A 30 cm radius of curvature, a 60° magnetic sector mass spectrometer was used. A secondary electron multiplier was used as the detector. Knudsen cell temperatures were measured by a disappearing filament optical pyrometer, calibrated against a standard NBS certified lamp. The pyrometer was sighted at a blackbody hole at the bottom of the cell. Appropriate window and prism corrections were applied.

The Al₂O₃ liner was inserted into a molybdenum cell. The effusion hole was 1 mm in diameter with an estimated Clausing factor of 0.4. Samples were prepared *in-situ* using MnF₂(s) with a molar equivalent of MnO(s) in the case of the OMnF and Mn₃O₄(s) for the study of the OMnF₂ molecule. Mn₃O₄(s) was produced by oxidizing pure MnO(s) in air at the temperature of 1050 °C.

The molecular beam effusing from the cell was ionized with 70 V electrons and the electron emission current was regulated at 1.0 mA. Identification of the ions was accomplished by the standard procedure.⁷ The intensities measured for the various ions were converted into partial pressures by

^{a)}Electronic mail: g.gigli@caspur.it

the relation $P = K f_i I_i^+ T$, where K is the instrument sensitivity constant and f_i a factor specific of the ion considered; f_i takes into account the cross section σ_i , multiplier gain γ_i , and isotopic abundance a_i of the specific ion, $f_i = 1/(\sigma_i \gamma_i a_i)$. An inverse square root dependence of the multiplier gain on the mass has been assumed for all the observed ions. The molecular ionization cross sections, σ_i , were evaluated, from the atomic values,⁸ by the method of Guido and Gigli.⁹ The resulting adopted values (in 10^{-16} cm²) for all the species taken into account are O₂ (3.13), Mn (6.75), MnO (6.35), MnF (6.21), MnF₂ (8.27), OMnF (8.01), and OMnF₂ (9.14).

The instrument sensitivity constant has been determined by the repeated quantitative evaporation of pure silver. The resulting value was 0.65 ± 0.08 bar K⁻¹ A⁻¹.

B. IR measurements

The experimental apparatus employed for matrix isolation measurements basically consists of Bruker IFS 113v interferometer under rotary vacuum and a cryotip (Air Products and Chemicals 202 CSA) rotatable in a home made shroud connected to a high-temperature furnace under high vacuum.

Blank spectra were collected for manganese tri- and difluoride vaporized from molybdenum Knudsen cells with orifices from 0.7 to 1.1 mm in the intervals 700–1000 K and 1000–1500 K, respectively. Preliminary vaporizations of manganese oxides (MnO, MnO₂ and Mn₃O₄) in the approximate range 800–1200 K were also performed. In the matrix deposition of Mn₃O₄ vaporization products, a very weak absorption at 833.5 cm⁻¹ was observed likely indicating the presence of a negligible amount of MnO.^{10,11} Other samples gave no bands in this region. Vaporizations of mixtures of manganese difluoride with Mn oxides were performed from a molybdenum Knudsen cell while a molybdenum double cell was employed when studying MnF₃ mixtures with MnO, MnO₂, and Mn₃O₄. The temperature gradient, around 200 K, was determined by the cell geometry. The fluoride was located in the colder compartment and its vapor was allowed to pass over the Mn oxide sample filling the hotter compartment of the cell itself. The vapors were deposited on a gold plated cold finger (12 K) in excess argon (Caracciolo, high purity). Depositions lasted from 5 to 60 min. A resolution of 1 cm⁻¹ or better was used.

III. RESULTS AND DISCUSSION

A. Mass spectrometric results

1. OMnF molecule

The experiments were typically performed by letting the system interact and degas for a couple of days at 850 °C before taking any measurement. Indeed, in the first stage of the evaporation process aluminum fluorides ions were found to be dominant in the effusing vapor. The ions identified by the usual procedure⁷ together with their appearance potential (in eV and determined by the vanishing current method) were ³²O₂⁺ (12.2), ⁴⁶AlF⁺ (17), ⁵⁵Mn⁺ (7), ⁶⁵AlF₂⁺ (15.5), ⁷¹MnO⁺ (7.5), ⁷⁴MnF⁺ (9.5), ⁸⁴AlF₃⁺ (14), ⁹⁰OMnF⁺ (10.5),

and ⁹³MnF₂⁺ (11.5). In all cases, the uncertainty in the appearance potential is 0.5 eV. The rather low value of the appearance potential of the OMnF⁺ ion is consistent with a simple ionization by electron impact.

The presence of the remaining ions ⁸⁴AlF₃⁺, ⁶⁵AlF₂⁺, ⁴⁶AlF⁺, ⁵⁵Mn⁺, ⁷⁴MnF⁺, and ⁹³MnF₂⁺, was attributed to the neutral precursors: AlF₃, Mn, MnF, and MnF₂, by analysis of the ionization efficiency curves together with the measured appearance potentials. A contribution of the dissociative ionization of MnF₂ to MnF⁺ must be taken into account, despite the fact that our experimental conditions produced an abundance of MnF⁺. Previous works provided spectra for the MnF₂ molecule.^{12–14} In Ref. 13, a detailed analysis of the electron impact mass spectra of the manganese fluorides was performed. For the MnF₂ molecule the ion intensities ratios, at 70 eV, were found to be as follows Mn⁺:MnF⁺:MnF₂⁺ = 36:100:38. This spectrum was later reproduced in Ref. 14. In contrast to the previous work, the present investigation resulted in a ratio between MnF⁺ and MnF₂⁺ ions, at 70 eV, that was smaller. Therefore, an experiment was performed with pure MnF₂(s) in a nickel cell that has been prefluorinated in order to prevent any interaction of the sample with the container material. Under these conditions no primary MnF⁺ was observed and the following ion intensities ratios have been measured: Mn⁺:MnF⁺:MnF₂⁺ = 14:84:100, leading to the conclusion that in our experimental conditions a smaller fragmentation occurs in the ion source. While these findings call for a full explanation, at the moment, it can only be pointed out that the difference in some feature of the ion sources could be the origin of this discrepancy. A possible explanation is the absence, in our ion source, of any magnet device that is sometimes used in order to increase the sensitivity. As a consequence, a larger proportion of molecules could follow the primary ionization channel in our apparatus. According to these observations, in the subsequent conversion of ion intensities into partial pressures, the measurements of the MnF⁺ and MnF₂⁺ ions have been corrected for the actual fragmentation pattern measured here.

2. OMnF₂ molecule

In addition to the ions reported above, the OMnF₂⁺ ion was also detected with an appearance potential of (10 ± 1) eV. No other possible precursors have been observed in the mass spectra. This, together with the value of the measured appearance potential, suggests the attribution of this ion to the primary ionization of the new molecular species OMnF₂. The possible contribution of the fragmentation by electron impact to the ion OMnF⁺ was not substantiated by these experiments. The ionization efficiency curves of the OMnF⁺ did not exhibit any upward break. In addition, it should also be mentioned that in the various stages of the experiments the ratio of the ion intensities OMnF₂⁺/OMnF⁺ varied rather largely. Indeed, in some cases no OMnF⁺ ion was detectable and, when observed, the ratio OMnF₂⁺/OMnF⁺ was found to range between 1.4 and 10.

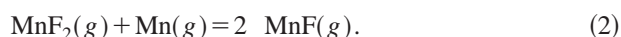
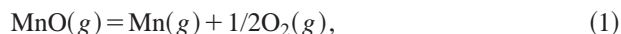
The measured intensities of the ions pertinent to this investigation are reported in Table I.

TABLE I. Ion intensities recorded in the experiments.

T/K	I(O ₂ ⁺)/A	I(Mn ⁺)/A	I(MnO ⁺)/A	I(MnF ⁺)/A	I(MnF ₂ ⁺)/A	I(OMnF ⁺)/A	I(OMnF ₂ ⁺)/A
1667	1.70E-11	1.55E-10			2.29E-11		
1781	5.10E-11	3.30E-09	2.05E-11	3.21E-11	7.58E-12	6.60E-12	
1789	5.20E-11	6.10E-10	3.80E-12	7.56E-12	1.86E-12		
1882	5.80E-10	1.70E-09	2.10E-11	1.07E-11		3.15E-12	
1962	3.70E-12	8.40E-09	6.85E-12	1.15E-11			
1892	4.20E-11	2.10E-09	7.65E-12	4.95E-12		3.90E-13	
1707		7.80E-10	1.60E-12		2.46E-10		
1719	2.40E-12	7.80E-10	1.30E-12		1.88E-10		
1741	1.40E-11	9.50E-10	3.35E-12	6.50E-11	1.26E-10		
1784	2.00E-11	1.95E-09	6.80E-12	6.24E-11	4.84E-11		
1832	3.00E-13	3.60E-08	1.25E-11	1.59E-10	1.46E-11	1.50E-12	
1845	1.40E-12	2.30E-08	1.75E-11	1.32E-10	1.53E-11	2.60E-12	
1865	4.45E-12	1.70E-08	1.70E-11	8.09E-11	7.25E-12		
1884	4.50E-12	1.45E-08	1.75E-11	6.01E-11	4.31E-12	1.60E-12	
1913		7.20E-09	1.50E-11	3.00E-11		1.30E-12	
1705	1.55E-10	3.10E-10	4.35E-12				
1735	9.60E-12	1.70E-09	6.25E-12	2.91E-11	1.53E-11	3.65E-12	5.10E-12
1772	4.00E-12	4.60E-09	7.00E-12	3.31E-11	7.63E-12	1.60E-12	2.10E-12
1767	2.40E-12	3.40E-09	4.50E-12	7.07E-12		3.10E-13	
1819	3.00E-12	5.75E-09	7.60E-12	2.94E-12		1.15E-13	1.15E-12
1861	9.40E-12	6.90E-09	1.25E-11	7.55E-12		3.60E-13	2.05E-12
1886	1.70E-11	9.15E-09	1.80E-11	6.76E-12		3.25E-13	1.35E-12
1911	2.15E-11	1.10E-08	2.40E-11	4.72E-12		2.40E-13	1.30E-12
1886	1.40E-11	9.15E-09	1.60E-11	3.35E-12		1.40E-13	2.00E-13
1857	1.45E-11	5.70E-09	1.00E-11	2.40E-12			

B. Thermochemical results

The nature of the condensed phase and the interaction with the container material caused a large variation in the gaseous phase composition during the vaporization experiments. Therefore, it was very important to reach equilibrium in the Knudsen cell and be able to check its attainment. At each temperature, measurements were taken after long equilibration times while continuously monitoring the intensity reproducibility of the ions of interest. In addition, the equilibrium constant of reactions involving known gaseous molecular species were measured, providing confidence in the attainment of equilibrium in the Knudsen cell. These reactions are



For reaction (1) it was possible to derive 22 equilibrium constants from the data in Table I and, hence, the so-called second- and third-law enthalpies. The second-law method, based on a least-squares analysis of $\ln K_p$ vs $1/T$ plots, provided a value of (129.2 ± 8.7) kJ mol⁻¹ at an average temperature of 1824 K. When reduced to 0 K the resulting II-law reaction enthalpy is (125.0 ± 8.7) kJ mol⁻¹. The corresponding third-law value, based on the relationship $\Delta_r H_0^\circ = -RT \ln K_p - T\Delta[(C_p^\circ - H_0^\circ)/T]$, is (118.5 ± 1.5) kJ mol⁻¹. From the average value of 121.8 kJ mol⁻¹ the atomization energy of the MnO molecule is derived to be $\Delta_a H_0^\circ(\text{MnO}, g) = 368.6$ kJ mol⁻¹, a value identical to the original one measured by Drowart and Smoes,¹⁵ (368.6 ± 7.5) kJ mol⁻¹, and in excellent agreement with the value tabulated in the Ivtanthermo database,¹⁶ 367.0 kJ mol⁻¹. In

performing these II- and III-law analyses, all the necessary thermodynamic functions and ancillary atomization enthalpies were taken from Ref. 16.

A similar analysis was performed for reaction (2). The necessary thermodynamic functions were taken, for consistency, from Ivtanthermo.¹⁶ The resulting third- and second-law enthalpies of reaction (2) were $\Delta_r H_0^\circ(\text{III-law}) = (100.3 \pm 1.5)$ kJ mol⁻¹ and $\Delta_r H_{1802}^\circ(\text{II-law}) = (100.6 \pm 18.7)$ kJ mol⁻¹; this last value, when reduced to 0 K provides $\Delta_r H_0^\circ(\text{II-law}) = (111.2 \pm 18.7)$ kJ mol⁻¹. Therefore, an average value of (105.8 ± 9.4) kJ mol⁻¹ can be proposed for this reaction and compared with the value of 87.1 kJ mol⁻¹ that can be obtained from the Ivtanthermo database atomization energies: $\Delta_a H_0^\circ(\text{MnF}_2, g) = 983.1$ kJ mol⁻¹ and $\Delta_a H_0^\circ(\text{MnF}, g) = 448$ kJ mol⁻¹. However, more recently the MnF₂ atomization energy has been redetermined¹⁷ as $\Delta_a H_0^\circ(\text{MnF}_2, g) = (995.6 \pm 5.0)$ kJ mol⁻¹. For consistency, a reanalysis of the original data has been made with the same thermodynamic functions employed in this investigation. By taking the average of the second- and third-law result, almost no variation is found in the final value for the atomization energy, $\Delta_a H_0^\circ(\text{MnF}_2, g) = (996.3 \pm 11.5)$ kJ mol⁻¹. With this new determination the enthalpy of reaction (2) is calculated to be 100.3 kJ mol⁻¹. Therefore, on one hand, our results are to be considered in agreement with previous studies and the outcome of the thermochemical analysis of this equilibrium gives confidence to the consistent use of the fragmentation pattern measured here. On the other hand, our results for reaction (2), together with the reanalysis that led to the aforementioned value of the enthalpy of atomization of MnF₂, allows us to propose a slightly revised downward value for

TABLE II. The Gibbs energy functions $-(G_T^\circ - H_0^\circ)/T$ (GEF_0), and enthalpy contents $H_T^\circ - H_0^\circ$ (HCF_0), for the gaseous molecules OMnF and OMnF₂.

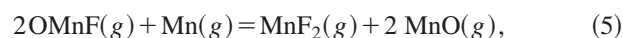
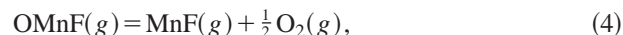
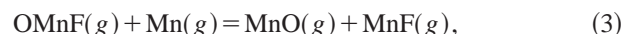
T/K	OMnF		OMnF ₂	
	GEF_0 J K ⁻¹ mol ⁻¹	HCF_0 kJ mol ⁻¹	GEF_0 J K ⁻¹ mol ⁻¹	HCF_0 kJ mol ⁻¹
298.15	231.645	12.889	258.101	14.943
1400	308.838	78.101	353.185	100.212
1500	312.701	84.259	358.147	108.387
1600	316.337	90.425	362.830	116.573
1700	319.773	96.600	367.263	124.773
1800	323.029	102.782	371.473	132.986
1900	326.123	108.969	375.479	141.209
2000	329.070	115.160	379.302	149.441
2100	331.885	121.356	382.956	157.681
2200	334.578	127.556	386.457	165.928
2300	337.159	133.759	389.817	174.180
2400	339.638	139.964	393.046	182.438

the MnF atomization enthalpy $\Delta_a H_0^\circ(\text{MnF}, g) = (445.2 \pm 7.4)$ kJ mol⁻¹.

1. OMnF molecule

In order to thermodynamically characterize this newly identified molecule, its thermodynamic functions, the Gibbs energy functions $-(G_T^\circ - H_0^\circ)/T$ (GEF_0) and the heat content functions $(H_T^\circ - H_0^\circ)$ (HCF_0), have been calculated by using the molecular parameters determined using quantum mechanical computations. The resulting values are reported in Table II.

From the measured ion intensities of Table I, the following all gas equilibria could be studied in the temperature range 1735–1913 K:



In principle, equilibria (3) and (4) as well as (5) and (6) are not independent, being related through the dissociation of the molecule MnO to atomic Mn and a molecular oxygen reaction (reaction 1). A similar observation applies to the coupled reactions (3)–(5) and (4)–(6). On the other hand, the set of points available for the study of the interrelated equilibria is not identical. Moreover, equilibria (3) and (5) are independent from the instrumental constant while (4) and (6) do depend on this parameter. Since systematic errors might have played a different role in the thermodynamic treatment of the data we preferred to study all of these equilibria.

The equilibrium constants and third-law data for all of the aforementioned reactions are reported in Table III. The drift in temperature of the third-law values is reported along with the average third-law enthalpy of reaction. This drift, evaluated by assuming a linear dependence of the individual points, provides a figure of merit for the absence of temperature trends. Also in Table III, the second-law enthalpy of reactions are reported. For equilibria (3) and (4), the selected enthalpies of the reaction are the average of the second- and third-law results. For the reactions (5) and (6), for which a

TABLE III. Equilibrium data and enthalpies^a for the reactions (3), (4), (5), and (6).

T/K	$\ln k_p(3)$	$\Delta_r H_0^\circ(3)/\text{kJ mol}^{-1}$	$\ln k_p(4)$	$\Delta_r H_0^\circ(4)/\text{kJ mol}^{-1}$	$\ln k_p(5)$	$\Delta_r H_0^\circ(5)/\text{kJ mol}^{-1}$	$\ln k_p(6)$	$\Delta_r H_0^\circ(6)/\text{kJ mol}^{-1}$
1781	-26.22	87.8	-52.28	207.5	-29.29	75.6	-81.4	315.0
1882	-23.49	86.9	-44.92	204.9				
1892	-22.69	85.8	-44.86	205.9				
1832	-24.58	86.9	-47.89	205.1	-27.30	73.7	-73.9	310.1
1845	-24.18	86.7	-47.57	206.0	-26.73	73.1	-73.5	311.6
1884	-22.85	85.8	-45.14	205.6	-25.36	71.8	-69.9	311.3
1913	-22.36	86.0						
1735	-26.48	86.2	-55.22	207.4	-27.84	71.4	-85.3	313.7
1772	-25.88	86.8	-50.84	203.9	-26.30	70.0	-76.2	304.2
1767	-26.23	87.2	-52.17	205.7				
1819	-25.29	87.7	-50.17	207.9				
1861	-24.32	87.6	-46.97	206.6				
1886	-23.70	87.5	-44.52	204.6				
1911	-23.31	87.7	-43.96	206.1				
1886	-23.52	87.1	-44.16	203.9				
	Avg. third law trend 10 ³	86.9 ± 0.7		205.8 ± 1.2		72.6 ± 2.0		311.0 ± 3.8
		-1.5		-7.5		5.7		-2.5
	Avg. temperature T/K	1843		1838		1807		1807
	Second Law $\Delta_r H_0^\circ$	77.5 ± 6.0		212.0 ± 11.0		48 ± 32		313 ± 63
	Second Law $\Delta_r H_0^\circ$	89.5 ± 6.0		219.7 ± 11.0		58 ± 32		317 ± 63
	Selected $\Delta_r H_0^\circ$	88.2 ± 3.0		212.8 ± 5.5		73 ± 15 ^b		311 ± 6 ^b
	Derived $\Delta_r H_0^\circ$ (OMnF)	902.0 ± 8.1		904.5 ± 9.2		903 ± 11		900 ± 6

^aErrors quoted are standard deviations.^bError estimated from the difference between the second- and third-law values.

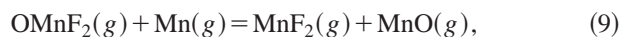
very limited number of experimental points could be taken, a second-law analysis is barely warranted. Nevertheless, we preferred to perform this analysis because it gives an idea of the quality of the primary data. Moreover, its deviation from the third-law value is used here as an estimate of the error on the selected value that is the third-law result. In the last row of Table III, the atomization energies of the OMnF molecule derived from the selected value of the various reactions are reported. In deriving these values the dissociation energy of MnO(*g*) was taken from Ref. 15 and the molecular oxygen dissociation energy from Ref. 16. The atomization energy of MnF₂, 996.3 kJ mol⁻¹, recalculated from Ref. 17, and the MnF atomization energy of MnF, 445.2 kJ mol⁻¹ proposed here, have been employed.

From the various values of $\Delta_a H_0^\circ(\text{OMnF}, g)$ presented in Table III, an overall average value of (903 ± 5) kJ mol⁻¹ is proposed for the atomization enthalpy of the OMnF molecule. This value was calculated by weighting the number of experimental points. The corresponding enthalpy of formation at 298.15 K, $\Delta_f H_{298.15}^\circ(\text{OMnF}, g) = (-297 \pm 5)$ kJ mol⁻¹ has been calculated by the pertinent thermochemical cycle using the ancillary data taken from Ref. 16.

2. OMnF₂ molecule

The molecular parameters needed to evaluate the thermodynamic functions of OMnF₂ were derived from the quantum mechanical calculations reported in Sec. III D. The computed GEF₀ and HCF₀ are reported in Table II.

Once again from the ion intensities of Table I, various equilibria can be taken into account in order to derive the atomization enthalpy of this species. The following reactions were considered:



Only two equilibrium constants at 1735 and 1772 K could be calculated for both reactions (8) and (9) yielding third-law reaction enthalpies of 223.2 and 231.5 kJ mol⁻¹ [reaction (8)], and 102.0 and 114.3 kJ mol⁻¹ [reaction (9)]. In the case of reactions (7) and (10), it has been possible to derive seven equilibrium points in the temperature range 1735–1911 K. However, the resulting third-law reaction enthalpy values were found to be quite scattered. The values ranged from 203.1 to 296.3 kJ mol⁻¹ for reaction (7) and from 116.9 to 208.5 kJ mol⁻¹ for reaction (10).

As a consequence of this scatter of the primary data, the range of possible values for the atomization energy of the OMnF₂ molecule varies between 1470 and 1543 kJ mol⁻¹, as it can be calculated with the appropriate thermochemical cycles when the necessary ancillary atomization energies for MnO¹⁵ and O₂,¹⁶ and for MnF and OMnF proposed here are used. Two simple remarks can be made on the reliability of these results. Within the measured range of values, smaller atomization energies were derived from those equilibrium points where the OMnF₂⁺ ion was found to be larger and, therefore, less prone to measurement errors. In addition, the

quantum mechanical computed atomization energy (see Section III D) supports a value at the lower end of the aforementioned range. In the situation depicted above a precise value cannot be given for the atomization energy of the OMnF₂ molecule, even if somewhat more credit should be given to the lower value, 1470 kJ mol⁻¹. Our best estimate of the possible uncertainty limit on this value is a rather large one: ± 70 kJ mol⁻¹. With the ancillary data of Ref. 16 the enthalpy of the formation at 298.15 K has been calculated to be $\Delta_f H_{298.15}^\circ(\text{OMnF}_2, g) = (-789 \pm 70)$ kJ mol⁻¹.

C. Vibrational frequencies

The infrared spectra of the vapors produced by MnF₃(*s*) and MnF₂(*s*) have been fully characterized in the past.^{18–22} A reinvestigation with our experimental apparatus was needed to study the spectroscopic behavior of the vapors over the mixture of MnF₃(*s*) and MnF₂(*s*) with manganese oxides.

Trapping the equilibrium vapor over manganese trifluoride, vaporized at 750 K in excess argon, two active infrared bands were detected at 758.6 and 711.4 cm⁻¹ and assigned to Mn–F stretching modes in agreement with previous observations.^{18,19} The spectrum is in agreement with the planar geometry with two longer and one shorter Mn–F bond (*C*_{2v} symmetry) suggested for the MnF₃ molecule by electron diffraction results.²³ When manganese trifluoride was heated at a temperature over 750 K, a band at 699.5 cm⁻¹ started to appear, indicating the presence in the vapor of manganese difluoride (our blank spectra and Refs. 18, 20, 21). This band gained intensity with the vaporization temperature and, at temperatures higher than 1200 K, was the only feature detected. Mixtures of MnF₂(*s*) and Mn oxides showed the appearance in the spectrum of the only former compound.

Mixtures of MnF₃(*s*) with Mn oxides were used for the spectroscopic investigation for two reasons. First, at the work vaporization temperature, MnF₂ was the main or the only species present in the vapor made to pass through the hotter part of the double crucible containing the Mn oxide as ascertained in the aforementioned preliminary vaporization of pure MnF₃(*s*). In fact, the fundamental modes of MnF₃ were never detected when vaporizing mixtures while the Mn–F stretching mode of the difluoride was always observed. Second, owing to the lower sensitivity of infrared apparatus with respect to the mass spectrometric one, a more efficient fluorination of Mn oxides was needed in order to achieve a higher concentration of oxyfluoride species in the vapor.

When trapping the equilibrium vapor over the mixture of MnF₃(*s*) and MnO(*s*) kept at 750 and 1200 K, the fundamental modes of MnF₂ were the only feature observed, suggesting the absence of a detectable amount of reaction products. Matrix spectra obtained when MnF₃ vapors were allowed to pass over MnO₂(*s*) or Mn₃O₄(*s*) were identical. In both cases new features were observed at 999.9, 988.4, 692.3, and 684.2 cm⁻¹. Neither the vaporization temperature nor the deposition time affected the intensity ratio of the new

TABLE IV. Optimized bond lengths (in Å), vibrational frequencies (in cm^{-1}), ZPE (in kJ mol^{-1}), atomization energies (in kJ mol^{-1}), and $\langle S^2 \rangle$ for the OMnF molecule computed at various levels of theory using the cc-pVDZ basis set for O and F, and then 6-31+G* basis set for Mn.

Method	State	$-E^a$	$r_{\text{Mn-O}}$	$r_{\text{Mn-F}}$	ν_1^b	ν_2	ν_3	ZPE	$\Delta_a H_0^\circ$	$\langle S^2 \rangle$
HF	$^1\Sigma$	1323.771 516	1.496	1.751	1258	144	703	13.5		0.000
HF	$^3\Sigma$	1323.878 099	1.706	1.833	685	<i>i</i> 57, 175	402			
HF	$^5\Sigma$	1324.052 603	1.834	1.843	705	112	577	9.00	696	6.012
HF	$^7\Sigma$	1324.049 941	1.875	1.826	727	140	570	9.43		12.00
MP2	$^1\Sigma$	1324.426 065	1.518	1.774	1154	88	659	11.9		0.000
MP2	$^3\Sigma$	1324.445 737	1.623	1.815	1301	<i>i</i> 48, 170	627			
MP2	$^5\Sigma$	1324.487 901	1.778	1.834	693	110	572	8.88	887	6.012
MP2	$^7\Sigma$	1324.242 354	1.871	2.309	615	93, 100	193	5.98		12.00
B3LYP	$^1\Sigma$	1325.931 706	1.520	1.737	1155	54, 72	706	11.9		0.000
B3LYP	$^3\Sigma$	1325.965 301	1.579	1.782	1004	<i>i</i> 48, 183	665			
B3LYP	$^5\Sigma$	1325.993 048	1.636	1.826	873	118	630	10.4	921	6.001
B3LYP	$^7\Sigma$	1325.992 714	1.892	1.793	719	88	573	8.79		12.00

^a E is in hartree.^b ν_1 and ν_3 are the stretching vibrational modes, and ν_2 is the bending vibrational mode.

bands suggesting their attribution to the same molecular species.

According to the KC-MS observations, the new bands observed could belong either to OMnF or OMnF₂ molecules. Since both species have a single Mn–O group, the bands at 999.9 and 988.4 cm^{-1} , lying in the spectral region where the Mn–O stretching mode is expected,^{10,11} can be interpreted as components of a doublet likely due to a matrix splitting effect. Remaining peaks at 692.3 and 684.2 cm^{-1} could also be considered a doublet, both in case of OMnF having a single Mn–F bond and also in case of OMnF₂, assuming that the second stretching mode is too weak to be detected. Alternatively, they can be attributed to the asymmetric and symmetric stretching modes of OMnF₂, respectively. The lack of fluorine isotopes does not allow an unequivocal assignment of the bands observed. However, a consideration of the fluorination efficiency of MnF₃ would seem to indicate the formation of OMnF₂.

The experimental frequency values are reproduced by the following force field: $F_{\text{Mn-O}}=7.16$; $F_{\text{Mn-F}}=4.03$; $F_{\text{O-Mn-F}}=0.26$; $F_{\text{F-Mn-F}}=0.057$; $F_{\text{MnF-MnF}}=0.68$; $F_{\text{MnO-MnF}}=0.4$; $F_{\text{OMnF-FMnF}}=0.0218$; $F_{\text{op}}=0.02$ mdyn/Å. These values are calculated assuming the Mn–O and Mn–F bond lengths of 1.5647 and 1.7291 Å, respectively, and a F–Mn–F angle of 118° in a planar arrangement, as sug-

gested by the quantum-mechanical calculations (see below). Undetected modes are also predicted: $\nu_3=183.3$; $\nu_5=320.9$, and $\nu_6=110.5$ cm^{-1} .

The frequencies calculated in the quantum mechanical section are reported in Tables IV and V for the OMnF and OMnF₂ molecules, respectively. A comparison of the predicted vibrational levels with the experimental observations leads to an assignment of the bands to the OMnF₂ molecule. In fact, the Mn–O stretching mode of OMnF₂ evaluated at 1016 cm^{-1} fits quite well the experimental value of the doublet at 999.9 and 988.4 cm^{-1} . However, calculations predict a gap around 100 cm^{-1} between the symmetric (a_1) and asymmetric (b_2) Mn–F stretching modes largely exceeding the distance between the bands detected in the Mn–F stretching region (692.3 and 684.2 cm^{-1}). On the grounds of the quantum mechanical results, therefore, it seems reasonable to assume that the bands at 692.3 and 684.2 cm^{-1} are components of a doublet attributable to the asymmetric stretching mode of OMnF₂ while the symmetric one is not visible as a consequence of its weak intensity. In this hypothesis, the expected higher intensity of the doublet attributed to the Mn–F stretching mode with respect to that one assigned to the Mn–O mode is in agreement with experimental observation. The overall picture is summarized in Table VI.

TABLE V. Optimized bond lengths (in Å), vibrational frequencies (in cm^{-1}), ZPE (in kJ mol^{-1}), atomization energies (in kJ mol^{-1}), and $\langle S^2 \rangle$ for the OMnF₂ molecule computed at various levels of theory using the cc-pVDZ basis set for O and F, and the 6-31+G* basis set for Mn.

Method	State	$-E^a$	$r_{\text{Mn-O}}$	$r_{\text{Mn-F}}$	$\angle \text{FMnF}^\circ$	b_1	a_1	b_2	a_1	b_2	a_1	ZPE	$\Delta_a H_0^\circ$	$\langle S^2 \rangle$
HF	2B_2	1423.286 811	1.843	1.719	103.9	337	227	530	660	820	800	20.2		0.777
HF	4A_2	1423.316 421	1.774	1.728	102.8	490	272	206	740	642	862	19.2		3.750
HF	4B_2	1423.529 217	3.003	1.831	180.0	132	48	30	569	735	132	9.85	961	5.299
HF	6B_2	1423.471 837	1.821	1.745	153.3	208	195	200	669	713	814	16.7		8.750
MP2	2B_2	1423.964 022	1.811	1.709	101.1	339	222	500	638	1905	789	26.3		0.777
MP2	4B_2	1424.158 102	1.710	1.745	106.5	201	204	210	696	791	1256	20.1	1279	4.007
MP2	6B_2	1424.131 338	1.809	1.750	159.0	189	188	181	651	790	701	16.1		8.750
B3LYP	2B_2	1425.756 421	1.785	1.719	100.3	219	211	37	629	704	761	15.3		0.798
B3LYP	4A_2	1425.788 538	1.791	1.714	118.3	525	181	119	648	739	753	17.7		3.750
B3LYP	4B_2	1425.907 222	1.565	1.729	118.1	158	192	263	671	782	1016	18.4	1405	3.754
B3LYP	6B_2	1425.864 896	1.798	1.749	160.1	160	177	145	646	782	699	15.6		8.750

^a E is in hartree.

TABLE VI. Experimental and calculated frequencies, in cm^{-1} , of the OMnF_2 molecule; in brackets IR intensities in km/mol .

	$\nu_1(a_1)$	$\nu_2(b_2)$	$\nu_3(a_1)$	$\nu_4(a_1)$	$\nu_5(b_2)$	$\nu_6(b_1)$
Exp	999.9 988.4	692.3		683.7		
B3LYP	1016 (95)	782 (147)	192 (9)	671 (46)	263 (5)	158 (49)
Normal coordinate analysis	988.6	693.1	183.3	684.1	320.9	110.5

D. Quantum-mechanical calculations

Ab initio and density functional calculations were carried out using the GAUSSIAN 98 electronic structure package.²⁴ These calculations were aimed at determining the molecular parameters and physical–chemical properties of the OMnF and OMnF_2 molecules.

Three levels of theory were used in this investigation: (i) the Hartree–Fock approach (HF), (ii) the second-order Møller–Plesset perturbation theory (MP2), and (iii) the density functional (DF) method using the Becke three-parameter exchange functional with the Lee, Yang, and Parr correlation functional (B3LYP). The basis sets employed for this study were a double- ζ polarized and diffuse basis set (6-31+G*) on manganese, and the correlated consistent polarized valence double- ζ basis set (cc-pVDZ) on oxygen and fluorine. The main purpose of these calculations is to provide reliable molecular parameters, bond lengths, and vibrational frequencies, to be used in the calculation of the thermal functions needed to evaluate the mass spectrometric equilibrium data and, consequently, the thermodynamic properties of OMnF and OMnF_2 .

In the evaluation of the thermal functions, we chose the molecular parameters computed at the B3LYP level of theory. To support our choice, we performed computations on the MnF and MnO molecules at the same level of theory employing the same basis sets. The computed molecular parameters agree with the experimental values; in particular, the bond distances, in Å, and the vibrational frequencies, in cm^{-1} , were calculated as 1.822 and 648 for MnF ; 1.627 and 903 for MnO . These computed bond distances are lower by 1.1%–1.3% than the experimental values, 1.843 Å for MnF , and 1.648 Å for MnO , whereas the computed vibrational frequencies are higher by 3.8%–7.5% than the experimental values, 624 cm^{-1} for MnF , and 840 cm^{-1} for MnO .

1. OMnF molecule

For the OMnF molecule, several configurations were explored, but only the computations for the global minimum (linear O–Mn–F) are reported. At all the levels of theory, the lowest-energy state was calculated to be a $^5\Sigma$. The Mn–O bond distance decreases from the HF to the B3LYP level of theory, becoming smaller by 0.198 Å; whereas the Mn–F bond length is approximately constant, varying by 0.017 Å with respect to the value calculated at the B3LYP level of theory. For the vibrational frequencies, there is a difference of approximately 170 cm^{-1} between the experimental and

calculated values of the Mn–O stretching mode reflecting the differences in the Mn–O distances. The Mn–F stretching mode values are almost constant with a 60 cm^{-1} higher Mn–F stretching at the B3LYP level of theory. The bending normal modes are within 10 cm^{-1} from each other.

Table IV lists the molecular parameters, zero-point vibrational energies (ZPE), the expectation values of the spin-squared operator ($\langle S^2 \rangle$), and the $\Delta_a H_0^\circ$ values of the OMnF molecule calculated at all the levels of theory employed. The $\Delta_a H_0^\circ$ have been calculated using the following relation: $\Delta_a H_0^\circ = E(\text{O}) + E(\text{Mn}) + E(\text{F}) - E(\text{OMnF}) - \text{ZPE}$, where E is the computed total energy. The computed atomization enthalpy, $\Delta_a H_0^\circ$, of 921 kJ mol^{-1} , is approximately 2% higher than the experimental value of 903 kJ mol^{-1} .

2. OMnF_2 molecule

For the OMnF_2 molecule, the lowest-energy geometry was found to have a C_{2v} symmetry. At all the levels of theory, the lowest-energy state was calculated to be a 4B_2 . At the HF level of theory the ground state is T-shaped, whereas at the MP2 and B3LYP levels the $\angle\text{F–Mn–F}$ angle varies from 106.5° to 118.1°. There is a large change in the Mn–O distance, decreasing from 3.003 Å at the HF level of theory to 1.565 Å at the B3LYP level. The Mn–F distance varies of 0.102 Å from the HF to the B3LYP method.

The $\langle S^2 \rangle$ value for the ground state is greater than that of the pure spin state, namely 3.75 for a quartet using MP2 and HF methods. This is essentially due to contamination by states of higher spin multiplicity, and, usually, for severely spin-contaminated wave functions the methods do not give reliable predictions.²⁵

Table V lists the molecular parameters, ZPE, $\langle S^2 \rangle$, and the $\Delta_a H_0^\circ$ values of the OMnF_2 molecule calculated at all the levels of theory employed. As already stated, the computed enthalpy of atomization of 1404 kJ mol^{-1} seems to support the experimental value at the lower end of the range.

In Table VI we see experimental and calculated frequencies of the OMnF_2 molecule.

¹M. J. Reisfeld, L. B. Asprey, and N. A. Matwiyoff, *Spectrochim. Acta*, Part A **27**, 765 (1971).

²A. K. Brisko, J. H. Holloway, E. G. Townson, and P. J. Levason, *J. Chem. Soc. Dalton Trans.* **11**, 3127 (1991).

³E. L. Varetti, R. R. Filgueira, and A. Mueller, *Spectrochim. Acta*, Part A **37**, 369 (1981).

⁴E. L. Varetti, *J. Raman Spectrosc.* **22**, 307 (1991).

⁵G. Balducci, M. Campodonico, G. Gigli, and S. Nunziante Cesaro, *Proceedings of HTMC-X*, in *Schriften des Forschungszentrums Juelich*, Reihe

- Energietechnik/Energy Technology, edited by K. Hilpert, F. W. Froben, and L. Singheiser, 2000, Vol. 15. Part II (Forschungszentrum Juelich GmbH, 2000, ISSN 1433-5522), p. 411.
- ⁶G. Balducci, P. E. Di Nunzio, G. Gigli, and M. Guido, *J. Chem. Phys.* **90**, 406 (1989).
- ⁷R. T. Grimley, in *The Characterization of High Temperature Vapors*, edited by J. L. Margrave (Wiley, New York, 1967), p. 195.
- ⁸J. B. Mann, in *Recent Developments in Mass Spectroscopy*, edited by K. Ogata and T. Hayakawa (University Park, Tokyo, 1980), p. 81.
- ⁹M. Guido and G. Gigli, *High. Temp. Sci.* **7**, 122 (1975).
- ¹⁰K. R. Thompson, W. C. Easley, and L. B. Knight, *J. Phys. Chem.* **77**, 49 (1972).
- ¹¹G. V. Chertihin and L. Andrews, *J. Phys. Chem.* **101**, 8547 (1997).
- ¹²R. A. Kent, T. C. Ehlert, and J. L. Margrave, *J. Am. Chem. Soc.* **86**, 5090 (1964).
- ¹³T. C. Ehlert and M. J. Hsia, *J. Fluorine Chem.* **2**, 33 (1972/1973).
- ¹⁴J. V. Rau, N. S. Chilingarov, M. S. Leskiv, A. V. Nikitin, L. N. Sidorov, S. V. Petrov, V. F. Sukhovkikhov, and Yu. F. Orekhov, *Russ. J. Phys. Chem.* **72**, 349 (1998).
- ¹⁵J. Drowart and S. Smoes, *High. Temp. Sci.* **17**, 31 (1984).
- ¹⁶*NIST-IVTANTHERMO Database of Thermodynamic Properties of Individual Substances*, developed in the Thermocentre Russian Academy of Science (CRC, New York, 1993).
- ¹⁷M. I. Nikitin, E. G. Rakov, V. I. Tsirel'nikov, and S. V. Khaustov, *Zh. Neorg. Khim.* **42**, 1154 (1997).
- ¹⁸S. B. Osin, D. I. Davlyatshin, V. F. Shevel'kov, and V. N. Mit'kin, *Russ. J. Chem.* **69**, 794 (1995).
- ¹⁹V. N. Buchmarina and Yu. B. Predtechenskii, *Opt. Spectrosc.* **80**, 684 (1996).
- ²⁰W. Hastie, R. H. Hauge, and J. L. Margrave, *High. Temp. Sci.* **1**, 76 (1969).
- ²¹J. W. Hastie, R. H. Hauge, and J. L. Margrave, *Chem. Commun.* **1969**, 1452.
- ²²A. Givan and A. Loewenschuss, *J. Chem. Phys.* **72**, 3809 (1980).
- ²³M. Hargittai, B. Réffy, M. Kolonits, C. J. Marsden, and J. Heully, *J. Am. Chem. Soc.* **119**, 9042 (1997).
- ²⁴M. J. Frisch, G. W. Trucks, H. B. Schlegel *et al.*, GAUSSIAN 98, Revision A.9, Gaussian, Inc., Pittsburgh, PA, 1998.
- ²⁵P. M. Mayer, C. J. Parkinson, D. M. Smith, and L. Radom, *J. Chem. Phys.* **108**, 604 (1998).

The Journal of Chemical Physics is copyrighted by the American Institute of Physics (AIP). Redistribution of journal material is subject to the AIP online journal license and/or AIP copyright. For more information, see <http://ojps.aip.org/jcpo/jcpcr/jsp>
Copyright of Journal of Chemical Physics is the property of American Institute of Physics and its content may not be copied or emailed to multiple sites or posted to a listserv without the copyright holder's express written permission. However, users may print, download, or email articles for individual use.

The Journal of Chemical Physics is copyrighted by the American Institute of Physics (AIP). Redistribution of journal material is subject to the AIP online journal license and/or AIP copyright. For more information, see <http://ojps.aip.org/jcpo/jcpcr/jsp>